ENERGY BUDGETS AND PERFORMANCE DEVELOPMENT OF TURBULENT BOUNDARY-LAYER CONTROL ON AIRFOILS

G. Fahland[1], *A. Stroh*[1], *D. Gatti*[1], *M. Atzori*[2], *R. Vinuesa*[2], *P. Schlatter*[2] *and B. Frohnapfel*[1]

[1] *Institute of Fluid Mechanics, Karlsruhe Institute of Technology (KIT), Karlsruhe, Germany*
[2] *SimEx/FLOW, KTH Engineering Mechanics, Royal Institute of Technology SE-100 44 Stockholm, Sweden*

georg.fahland@kit.edu

Abstract

We present a comprehensive parametric study on the flow-control scheme denoted as wall-normal uniform blowing and suction in turbulent boundary layers around airfoils. The focus is primarily put on the influence of the drag caused by the power consumption of the support system. We also assess the theoretical background of the momentum budget including free-stream and boundary-layer control flux. It is shown that this assessment is crucial if a complete understanding and a reliable measurement of the drag in such system is desired in practice.

1 Introduction

Despite the sizeable impact of the COVID-19 pandemic on air-traffic development the need for emission reduction by drag reduction remains crucial for the decades to come. Aircraft design still has many possibilities for efficiency improvement despite the huge efforts in the past in fields like engine design and lightweight construction. Viscous drag reduction by boundary layer control (BLC) is a field which is lacking wide-spread implementation despite some efforts on implementing laminar boundary layer control on newest generation aircraft tailplanes. This lack of implementation is even more severe for turbulent boundary layer control although the turbulent state is often unavoidable for commercial aircraft given the high Reynolds numbers, swept wings, flap design, manufacturing imperfections such as rivets and leading edge deposits like bugs, dirt, etc. This justifies increased efforts in investigating turbulent boundary layer control schemes. We focus on the active scheme of uniform blowing as it is a simple scheme quite a few experimental [11, 6, 4, 9] and numerical [8, 14, 2] investigations exist for. It also allows to build on the experience of laminar flow-control regarding the actual implementation on aircraft [13]. Furthermore it could be shown that the drag reduction potential is significant given a favourable use case can be identified. [5]. For example, large potential is recognized in the scheme of blowing on the pressure side (PS) of an airfoil within the turbulent region at favourable or mildly adverse pressure gradients like they exist on cambered airfoils at lower angles of attack. In this presentation and proceeding we focus on the energy budget calculation including the control scheme power requirements as well as how to correctly assess the total drag based on the momentum budget equation.

2 Methodology

The incompressible Reynolds-Averaged Navier-Stokes (RANS) equations are solved with the SIMPLE FOAM solver from OpenFOAM. Menter $k\omega$-SST [10] is set as turbulence model. Upstream of $x/c = 10\%$, with c being the chord length, the turbulent kinetic energy (TKE) is kept at practically zero to simulate a laminar boundary layer. The mesh resolution is sufficient to allow low-Re modeling *i.e.* $y^+ \leq 1$ for the first cell at the wall. The mesh is C-shaped with a radius of 50 airfoil chord lengths, c. The outlet is $75c$ behind the trailing edge of the airfoil. On the surface of the airfoil a no-slip condition is imposed in the uncontrolled regions. For controlled regions a uniform wall-normal velocity is prescribed. The setup of simulations, boundary conditions and variation of parameters correspond to the ones reported in Fahland *et al.* [5]. Validation of the setup is done with LES data from Atzori *et al.* [2].

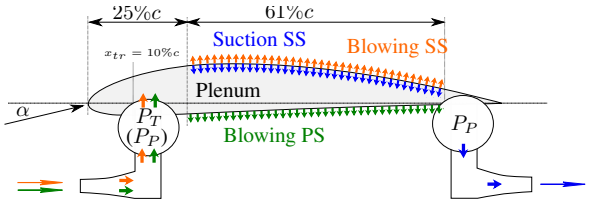

Figure 1: Control schemes and schematics of the system providing the flow-control mass flux

The flow-control schemes investigated within the present parametric study are displayed in figure 1. The upper side of the airfoil is referred to as suction side (SS) while the lower side of the airfoil is labelled as pressure side (PS) no matter whether blowing or suction is applied. The parametric study covers the fol-

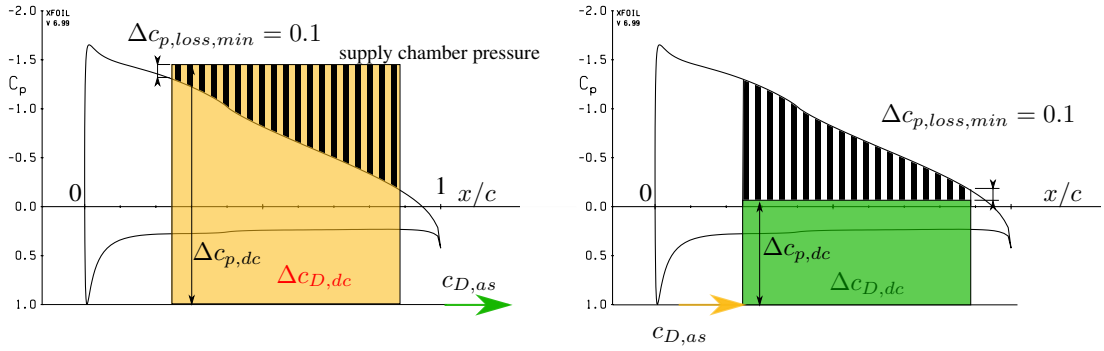

Figure 2: Power consumption of a suction scheme (left) and of a blowing scheme (right) on the upper side of an airfoil in dimensionless visualisation. Green items indicate specific drag savings e.g. thrust, orange items show additional drag

lowing variations for the NACA 4-digit airfoil family:

- angle of attack (AoA) $\alpha = [-3, 12]°$
- Reynolds number based on chord $Re_C = [1e5, 4e6]$
- BLC velocity $v_{BLC} = [0.1, 0.5]\%U_\infty$
- airfoil thickness $t = [6, 15]\%c$
- airfoil camber $f = [0, 6]\%c$

Figure 1 also shows how the boundary-layer control fluid is gathered from (in case of a blowing scheme) or discharged to free stream. In principle, both could take place at ambient pressure leaving no penalty for this process. In reality the amounts of fluid are considerably large and it is impossible for an aircraft to carry it along at ambient pressure. Therefore, the fluid meant for blowing has to be gathered at free-stream conditions implying an inevitable momentum loss (although no energy is lost at this moment if one assumes that the fluid is gathered at a stagnation point). This results in a drag component for the air supply $c_{D,\mathrm{as}}$. Meanwhile for suction schemes the opposite is true as pointed out by Beck *et al.* [3]. The discard of non-moving fluid in the reference frame of the aircraft can take place at e.g. free-stream velocity. Although one has to provide the necessary pressure difference for this, doing so is highly desirable since the propulsive efficiency of this exhaust is 100%. This results in a negative drag component $c_{D,\mathrm{as}}$ for the air discharge in case of a suction scheme.

For both cases (blowing and suction scheme) the pressure level of the air supply (or discharge) is assumed at free-stream total pressure (dimensionless static pressure $c_p = (p - p_\infty)/(\rho/2u_\infty^2) = 1$) in order to allow discharge or collection at free-stream conditions. Figure 2 shows the pressure differences which have to be overcome to get to the BLC surface. Since one has to distribute the BLC-fluid evenly without an extensive hardware overhead a distribution scheme of tailored losses is most practical (e.g. Scholz *et al.* [12]). This results in an achievable pressure level at the supply chamber (plenum) of at least $\Delta c_{p,\mathrm{loss,min}} = 0.1$ [3] higher than the highest airfoil surface pressure in the BLC region in case of blowing (equivalently lower in case of suction). In figure 2 the distribution losses are indicated by the black bars. The corresponding power is assumed to be lost completely. Consequently, a plenum pressure level can be formulated for each case. The pressure difference to the air supply/discharge at $c_p = 1$ is then to be overcome using a pump (in case of suction) or a small turbine (in case of blowing). The drag associated to the power consumption (P_P in case of a pump) or power generation (P_T in case of a turbine) of these items has to include a corresponding efficiency which is set to be $\eta = 70\%$ following the suggestion by Beck *et al.* [3].

In total the drag related to the BLC hardware consists of the two described portions: the momentum loss due to air supply/discharge and the pump/turbine power. They can be recast in terms of dimensionless drag coefficients as shown in equation 1. Doing so, the aerodynamic drag coefficient $c_{d,\mathrm{aero}}$ can be corrected to include the BLC system drag as $c_{d,\mathrm{corr}}$:

$$c_{d,corr} = c_{d,aero} + \underbrace{\begin{cases} \text{pump:} & \frac{1}{\eta_P}\frac{|v_{\mathrm{BLC}}|}{U_\infty}\frac{l_{\mathrm{BLC}}}{c}\Delta c_p \\ \text{turbine:} & -\eta_T\frac{|v_{\mathrm{BLC}}|}{U_\infty}\frac{l_{\mathrm{BLC}}}{c}\Delta c_p \end{cases}}_{\text{providing/harvesting pressure difference}} + \underbrace{\begin{cases} \text{suction:} & -\frac{|v_{\mathrm{BLC}}|}{U_\infty}\frac{l_{\mathrm{BLC}}}{c} \\ \text{blowing:} & \frac{|v_{\mathrm{BLC}}|}{U_\infty}\frac{l_{\mathrm{BLC}}}{c} \end{cases}}_{\text{Momentum gain/loss to free-stream}}, \tag{1}$$

The improvement of a controlled case is measured as drag reduction compared to the uncontrolled case at equal lift coefficient c_l. It is important not to compare the drag reduction at equal angle of attack due to the fact that a certain drag reduction can also coincide with

a lift reduction similar to e.g. flap deflections. Yet this does not necessarily offer any efficiency benefit in a real-world application. For an actual benefit the airfoil polar (as seen in figure 3) has to be shifted to the left.

3 Results

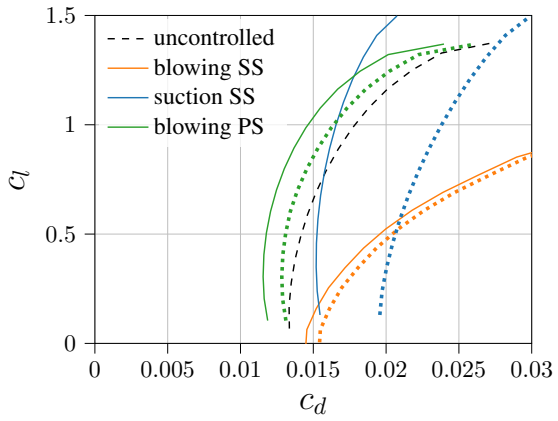

Figure 3: Polar plot of the following cases uniform blowing on the SS, uniform suction on the SS and uniform blowing on the pressure side. The parameters are $v_{BLC} = 0.5\%U_\infty$, $Re_C = 4 \cdot 10^5$, NACA 4412.

The polar plot in figure 3 shows that the schemes of uniform blowing on the PS and uniform suction on the SS both can yield an improvement compared to the uncontrolled polar: at least parts of the corresponding polars are shifted to the upper left from the uncontrolled reference. For suction on the SS the aerodynamic improvement exists for higher lift coefficients like present upon aircraft launch and approach. This is also why it is not a significant disadvantage that the polar with included energy budget is significantly shifted to higher drag. The system is needed for small parts of the total flight time only at the benefit of reducing wing area thanks to higher $c_{l,\max}$, which in turn improves the efficiency during cruise. For blowing on the PS the situation is different. An increase in maximum lift can barely be expected. Hence the improvement has to be reached directly. Due to the smaller system drag which results from the much smaller pressure differences observed in figure 2 a net gain can be reached for medium lift coefficients. Although the energy consumption of blowing on the SS is even lower than that of blowing on the PS due to the more favourable pressure difference, the detrimental aerodynamic performance of such a configuration cannot be compensated.

Regarding the trends with Reynolds number (figure 4) it becomes apparent that the relative energy consumption of a BLC system rises with higher Re. This can be explained by the Re-independent losses assumed within the system which stay constant at any Re in their dimensionless value. Meanwhile, the aerodynamic performance of any airfoil in a strictly turbulent regime rises due to the reduced viscous effects.

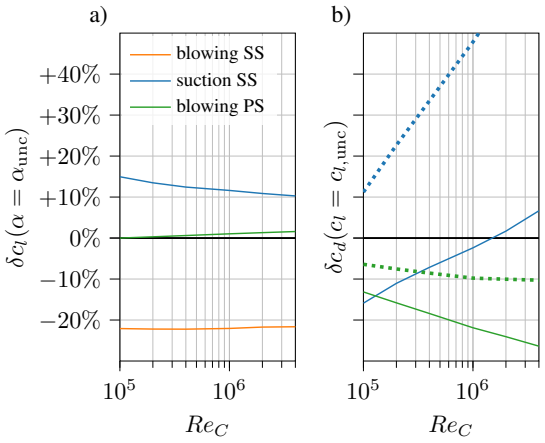

Figure 4: Development of aerodynamic coefficients and efficiency improvement relative to the uncontrolled polar. Operating point: NACA 4412, $\alpha = 5°$ for the BLC case (equal lift for the uncontrolled case), $v_{\mathrm{BLC}} = 0.5\%U_\infty$

This in turn has the effect that the aerodynamic drag portion drops compared to the BLC system drag. In total we see a reduction of the aerodynamic drag in the case of blowing on the PS savings for higher Re_C, while the corrected drag savings for the scheme of blowing on the PS saturates. Suction on the SS has a declining aerodynamic performance at a fixed AoA since rising Re reduces the boundary layer growth so the suction cannot yield a significant improvement. Including the BLC drag renders this effect even worse due to the aforementioned reasons.

In the following we focus on the scheme of blowing on PS since it is the only one considered with direct overall drag reduction. Figure 5 shows how its performance changes with the camber of an airfoil f and Re. For $\alpha = 0$ and symmetric airfoils it becomes clear that no improvement can be reached including the system drag. The slight aerodynamic improvements of approximately 5% in the presence of an adverse pressure cannot compensate the cost of the BLC system. This is an important finding since symmetric airfoils are very common for experimental test campaigns [9] or first implementations on aircraft due to the smaller effort modifying a tailplane compared to a wing [13]. However, the higher the camber the more favourable the pressure gradient on the PS so a drag reduction is present. The same trend as in figure 4 becomes visible. Whereas the improvement of the plain aerodynamic values still continues for the highest Re the net improvement saturates at around $\delta c_l = -10\%$. At higher AoA the pressure gradient on the PS is more favourable in general so an improvement already exists for symmetric airfoils. Also the maximum improvement is slightly higher at $\alpha = 5°$ which correlates well with the polar plot observations (figure 3).

At this point it is interesting to understand the cause of the observed drag reduction. Clearly, a reduc-

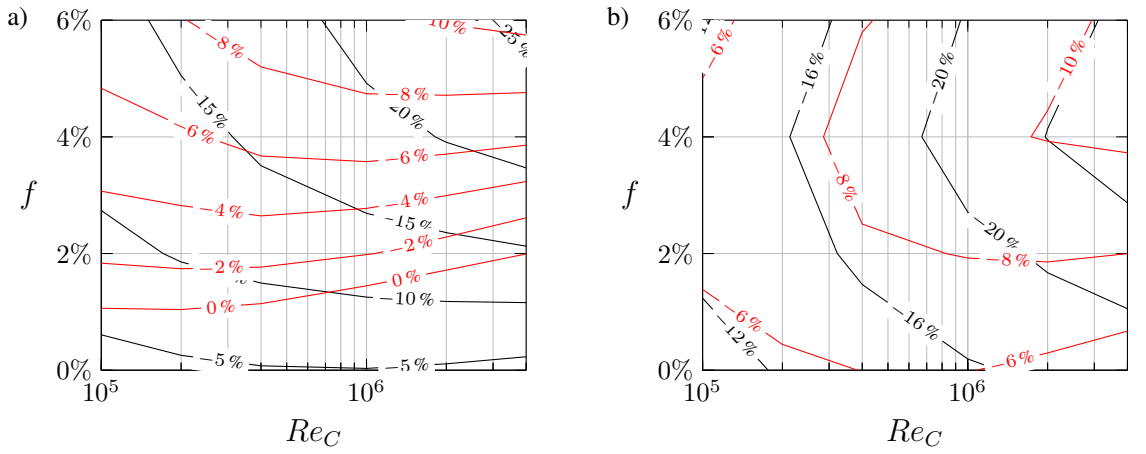

Figure 5: Drag reduction for equal c_l as the corresponding uncontrolled case at $\alpha = 0°$ (a) and at $\alpha = 5°$ (b) as function of airfoil camber f and Reynolds number Re. Plain aerodynamic comparison is plotted in black, BLC-system drag results are plotted in red.

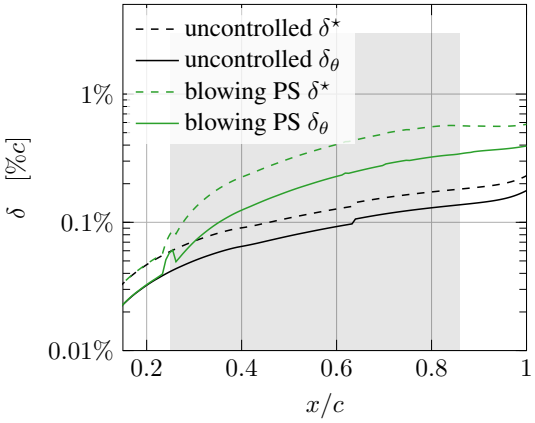

Figure 6: Boundary-layer development on the pressure side of NACA 4412, $v_{BLC} = 0.5\%U_\infty$, $\alpha = 5°$. Both the momentum thickness (δ_θ) and the displacement thickness ($\delta^\star$) rise within the BLC region (grey area) compared to the uncontrolled case.

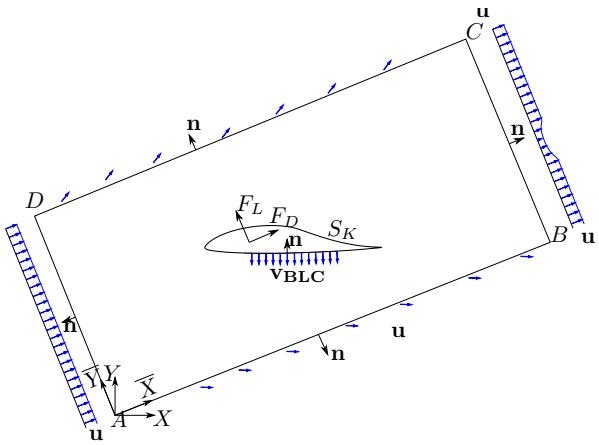

Figure 7: Control Volume (CV) for 2D airfoil momentum assessment in which $\mathbf{n}$ is the normal vector pointing out of the CV.

tion in friction drag is present due to the effects similarly observed in zero pressure gradient boundary layers [7, 8, 14]. However, as figure 6 shows, this comes at the cost of an increased boundary layer thickness, both for the momentum loss δ_θ and the displacement thickness $\delta^\star$. Contrary to intuition, the larger boundary layer thickness does not necessarily cause a pressure drag increase although the momentum deficit in the controlled case at the trailing edge is larger due to the thicker boundary layer. Especially for the most advantageous blowing on the PS conditions a slight decrease in pressure drag contributes to the overall drag reduction. This apparent contradiction is addressed in the following.

4 Theoretical Analysis of the Drag Reduction

Here we investigate how it is possible that the total drag (and in some cases even the pressure drag) of an airfoil drops although the thickness of the boundary layer and thus the momentum deficit in the wake rises. Changing the perspective, an airfoil of which all the boundary layer is sucked off completely experiences no momentum deficit in the wake, yet the airfoil still experiences drag. In this case the momentum loss of the fluid which got sucked in is responsible for the entire drag also called the sink-drag. Note that the drag force is transferred to the airfoil by both wall friction and pressure drag at the orifices in the wall where the last stream-wise velocity component of the suction fluid is removed. Accordingly, the opposite effect takes place for blowing: Although the source is not directed towards the rear of the airfoil and the

deficit in the wake is larger than for the uncontrolled case there is a thrust term originating in this source as can be shown considering the momentum budget. This is discussed in detail in the supplemental material of Fahland *et al*. [5]. We recapitulate this topic here.

The momentum budget for the control volume in figure 7 is given as:

$$\underbrace{\iint\limits_{(S)} \rho\mathbf{u}(\mathbf{u}\cdot\mathbf{n})dS}_{\text{momentum flux}} = \underbrace{\iint\limits_{(S)} \mathbf{t}dS}_{\text{forces on control volume boundaries}} \quad , \quad (2)$$

The right-hand side of the equation is not altered by the boundary-layer control:

$$\iint\limits_{(S)} \mathbf{t}dS = \underbrace{\iint\limits_{\overline{ABCD}} \tau(\mathbf{n}\times(0,0,1)^T)dS}_{\text{shear forces on CV outer box}=0} + \underbrace{\iint\limits_{\overline{ABCD}} -p\mathbf{n}dS}_{\text{pressure forces box}} + \underbrace{\begin{bmatrix}-F_D\\-F_L\\0\end{bmatrix}_{\{\overline{X},\overline{Y},\overline{Z}\}}}_{\text{Forces on airfoil in stability axis}} \quad (3)$$

However, the left-hand side does experience an alteration since there is a mass flux over the surface of the airfoil.

$$\iint\limits_{(S)} \rho\mathbf{u}(\mathbf{u}\cdot\mathbf{n})dS = \underbrace{\iint\limits_{\overline{ABCD}} \rho\mathbf{u}(\mathbf{u}\cdot\mathbf{n})dS}_{\text{Flux outer box}} + \underbrace{\iint\limits_{S_K} \rho\mathbf{v_{BLC}}(\mathbf{v_{BLC}}\cdot\mathbf{n})dS}_{\text{Flux crossing airfoil surface}} \quad (4)$$

A solution of the $\overline{X}$-component of these equations for the drag force F_D delivers for a 2D airfoil:

$$\frac{F_D}{z} = \rho U_\infty^2 \Bigg(\underbrace{\int\limits_B^C \frac{u_{\overline{X}}}{U_\infty}\left(1-\frac{u_{\overline{X}}}{U_\infty}\right)d\overline{Y}}_{\text{wake momentum deficit}} \underbrace{-\frac{v_{BLC}}{U_\infty}l_{BLC}}_{\text{BLC thrust}} \Bigg) \quad (5)$$

In the case of an uncontrolled airfoil the drag can be evaluated by measuring the momentum deficit of the wake only as done in many experiments (e.g. [1]). However, to get the correct measurement of the controlled airfoil one has to take into account the mass flux of the control.

In contrast to the free-stream the BLC fluid enters the domain with almost zero momentum. Yet it gets deflected and exits the control volume with a non-zero momentum. This gain in momentum is also drawn from the free-stream but does not add up to the drag of the airfoil although causing a momentum deficit its wake. This effect is responsible for the total drag reduction (and also for the pressure drag reduction if present) despite the thicker boundary layers in the controlled case.

To put this into perspective, it is important to remember that the effect described here comes at the cost of previously lost momentum when collecting the fluid from the free-stream, which is later expelled as BLC fluid. However, this momentum loss was already accounted for as air-supply drag $c_{D,\mathrm{as}}$ in the BLC-system drag as shown in section 2, figure 2.

5 Conclusions

Results of a large parametric study on turbulent 2D airfoil flows with wall-normal uniform suction and blowing using RANS are presented. In the present work we focus on the assessment of the drag components related to the system providing the control scheme. It is shown that this has a strong influence on the overall performance development assuming a conservative yet universal set of system parameters. Although the improvement of some of the aerodynamically advantageous control schemes is reduced when the overall performance is considered, a positive net effect can be identified for the most of these schemes. We note that this conclusion also strongly depends on the use case. At equal lift coefficient aerodynamic drag reduction of approximately 30% can be realized within the investigated parameter space. At the same time the net drag savings at equal lift coefficient still reach more than 10%.

The present numerical study is highly relevant for the design of experimental investigations for active control on airfoils. The generated data allow for estimation at which operating conditions an adequate signal to noise ratios can be expected in order to achieve experimental proof of concept for realization of net performance increase due to turbulent boundary-layer control through blowing and suction.

Acknowledgments

GF, DG, BF and AS acknowledge support by the state of Baden-Württemberg through bwHPC. MA, RV and PS acknowledge financial support from the Swedish Foundation for Strategic Research, project "In-Situ Big Data Analysis for Flow and Climate Simulations" (ref. number BD15-0082), from the Knut and Alice Wallenberg Foundation and from the Swedish Research Council (VR). The simulations were performed on resources provided by the Swedish National Infrastructure for Computing (SNIC) and within the project CWING on the national supercomputer Cray XC40 Hazel Hen at the High Performance Computing Center Stuttgart (HLRS).

References

[1] D. Althaus. *Niedriggeschwindigkeitsprofile: Profilentwicklungen und Polarenmessun-*

gen im Laminarwindkanal des Instituts für Aerodynamik und Gasdynamik der Universität Stuttgart. ger eng. OCLC: 845149238. Braunschweig: Vieweg, 1996. ISBN: 978-3-528-03820-5.

[2] M. Atzori et al. "Aerodynamic Effects of Uniform Blowing and Suction on a NACA4412 Airfoil". en. In: *Flow Turbulence Combust* 105 (Apr. 2020), pp. 735–759. ISSN: 1386-6184, 1573-1987. DOI: 10.1007/s10494-020-00135-z. URL: http://link.springer.com/10.1007/s10494-020-00135-z (visited on 04/29/2020).

[3] N. Beck et al. "Drag Reduction by Laminar Flow Control". en. In: *Energies* 11.1 (Jan. 2018), p. 252. ISSN: 1996-1073. DOI: 10.3390/en11010252. URL: http://www.mdpi.com/1996-1073/11/1/252 (visited on 09/26/2019).

[4] Kaoruko Eto et al. "Assessment of Friction Drag Reduction on a Clark-Y Airfoil by Uniform Blowing". en. In: *AIAA Journal* 57.7 (July 2019), pp. 2774–2782. ISSN: 0001-1452, 1533-385X. DOI: 10.2514/1.J057998. URL: https://arc.aiaa.org/doi/10.2514/1.J057998 (visited on 06/22/2021).

[5] G. Fahland et al. "Investigation of Blowing and Suction for Turbulent Flow Control on Airfoils". In: 0.0 (July 2021), pp. 1–15. DOI: 10.2514/1.J060211. URL: https://doi.org/10.2514/1.J060211 (visited on 07/05/2021).

[6] Marco Ferro. "Experimental study on turbulent boundary-layer flows with wall transpiration". English. ISBN: 9789177295563 OCLC: 1023294987. PhD thesis. Stockholm: KTH Royal Institute of Technology, 2017. (Visited on 06/15/2021).

[7] D. Hwang. "Review of research into the concept of the microblowing technique for turbulent skin friction reduction". en. In: *Progress in Aerospace Sciences* 40.8 (Nov. 2004), pp. 559–575. ISSN: 03760421. DOI: 10.1016/j.paerosci.2005.01.002. URL: https://linkinghub.elsevier.com/retrieve/pii/S0376042105000096 (visited on 05/07/2020).

[8] Y. Kametani and K. Fukagata. "Direct numerical simulation of spatially developing turbulent boundary layers with uniform blowing or suction". en. In: *J. Fluid Mech.* 681 (Aug. 2011), pp. 154–172. ISSN: 0022-1120, 1469-7645. DOI: 10.1017/jfm.2011.219. URL: https://www.cambridge.org/core/product/identifier/S0022112011002199/type/journal_article (visited on 06/25/2020).

[9] V. Kornilov. "Combined Blowing/Suction Flow Control on Low-Speed Airfoils". en. In: *Flow Turbulence Combust* 106.1 (Aug. 2020), pp. 81–108. ISSN: 1386-6184, 1573-1987. DOI: 10.1007/s10494-020-00157-7. URL: http://link.springer.com/10.1007/s10494-020-00157-7 (visited on 08/31/2020).

[10] F. Menter. "Zonal Two Equation k-w Turbulence Models For Aerodynamic Flows". en. In: *23rd Fluid Dynamics, Plasmadynamics, and Lasers Conference*. Orlando,FL,U.S.A.: American Institute of Aeronautics and Astronautics, July 1993. DOI: 10.2514/6.1993-2906. URL: http://arc.aiaa.org/doi/10.2514/6.1993-2906 (visited on 02/07/2020).

[11] H. S. Mickley. "Heat, mass, and momentum transfer for flow over a flat plate with blowing or suction". In: *NACA, TN 3208* (1954), pp. 1–25.

[12] P. Scholz. *Simulation of Pressure Losses for the Design of Tailored Suction Distributions for Laminar Flow Control*. engl. Cambridge, UK, Mar. 2015. URL: http://edrfcm-2015.eng.cam.ac.uk/pub/EDRFCM2015/MeetingProgram/56_Scholz.pdf (visited on 05/13/2020).

[13] G. H. Schrauf and H. von Geyr. "Simplified Hybrid Laminar Flow Control for the A320 Fin - Aerodynamic and System Design, First Results". en. In: *AIAA Scitech 2020 Forum*. Orlando, FL: American Institute of Aeronautics and Astronautics, Jan. 2020. ISBN: 978-1-62410-595-1. DOI: 10.2514/6.2020-1536. URL: https://arc.aiaa.org/doi/10.2514/6.2020-1536 (visited on 06/25/2020).

[14] A. Stroh et al. "Global effect of local skin friction drag reduction in spatially developing turbulent boundary layer". en. In: *J. Fluid Mech.* 805 (Oct. 2016), pp. 303–321. ISSN: 0022-1120, 1469-7645. DOI: 10.1017/jfm.2016.545. URL: https://www.cambridge.org/core/product/identifier/S0022112016005450/type/journal_article (visited on 07/06/2020).